



# Fiber Metal Laminates Based on Natural/Synthesis Fiber Composite for Vehicles Industry: an Experimental Comparative Study

Mahmoud M. Awd Allah<sup>1</sup> · Dalia A. Hegazy<sup>2</sup> · Hassan Alshahrani<sup>3</sup> · Tamer A. Sebaey<sup>1,4</sup> · Marwa A. Abd El-baky<sup>1</sup>

Received: 27 May 2023 / Revised: 16 June 2023 / Accepted: 24 June 2023 / Published online: 17 July 2023  
© The Author(s), under exclusive licence to the Korean Fiber Society 2023

## Abstract

Fiber metal laminates (FMLs) are made by sandwiching a fiber-reinforced composite between thin layers of metals. FMLs are the most modern materials utilized in automotive and aerospace manufacture because of their superior mechanical behavior when compared to conventional metallic alloys. In the current work, the effect of hybridization between jute-reinforced composites and other fabrics on the mechanical properties of the designed FMLs was experimentally assessed under various tests, including tension, flexural, in-plane shear, interlaminar shear, and bearing tests. Aluminum alloy 1050 (AA 1050) was used as a metal component in the designed FMLs, while the composite components are jute (J), glass (G), aramid (A), carbon (C), and basalt (B) fabrics. To ensure good adhesion between Al-sheets and composite laminates, Al-sheets underwent both mechanical and chemical treatments. The intended FMLs were prepared via hand lay-up and compression casting techniques. The designed stacking sequences were 8 J, 2G/4J/2G, 2A/4J/2A, 2C/4J/2C, and 2B/4J/2B. According to the experimental results compared with the 8 J specimen, the 2G/4J/2G specimen presents maximum flexural strength, flexural modulus, and interlaminar shear strength with an improvement percent of 51.51, 212.33, and 15.72%, respectively. On top of that, the 2A/4J/2A specimen introduces maximum tensile failure strain and tensile toughness modulus with an enhancement percent of, respectively, 21.56 and 116.56%, while the 2C/4J/2C specimen introduces extreme tensile strength, tensile modulus, flexural strain, in-plane shear strength, and bearing strength with an upgrading percent of 181.91, 111.86, 21.24, 26.38, and 60.94%, respectively.

**Keywords** Mechanical properties · Fiber metal laminates (FMLs) · Natural/synthesis hybrid fabrics · Specimen failure · Vehicle applications

## List of Abbreviations

FMLs	Fiber metal laminates
AA 1050	Aluminum alloy 1050
Al	Aluminum
J	Jute fabrics
G	Glass fabrics
A	Aramid fabrics

C	Carbon fabrics
B	Basalt fabrics
F	Flax fabrics
K	Kenaf fabrics
CAFRALL	Laminates made from carbon and flax fiber-reinforced aluminum
CAKRALL	Laminates made from carbon and Kenaf fiber-reinforced aluminum
EFFMLs	Eco-friendly fiber metal laminates
HCl	Hydrochloric acid
NaOH	Sodium hydroxide
UTM	Universal testing machine
$\sigma_{ult}$	Ultimate tensile strength
$E_{app}$	Apparent tensile modulus
$U_T$	Toughness modulus
$\sigma_{fl}$	Flexural strength
$\epsilon_{fl}$	Flexural strain
$E_{fl}$	Flexural modulus
$\tau_{12}$	In-plane shear stress

✉ Marwa A. Abd El-baky  
dr.marwa2013@yahoo.com

<sup>1</sup> Mechanical Design and Production Engineering Department, Zagazig University, Sharqia, Egypt  
<sup>2</sup> Bilbeis Higher Institute of Engineering (BHIE), Bilbeis, Sharqia, Egypt  
<sup>3</sup> Department of Mechanical Engineering, College of Engineering, Najran University, Najran, Saudi Arabia  
<sup>4</sup> Engineering Management Department, College of Engineering, Prince Sultan University, Riyadh, Saudi Arabia

ILSS	Interlaminar shear strength
SBS	Short beam shear
$\sigma_b$	Bearing strength

## 1 Introduction

Fiber metal laminates (FMLs) are a class of hybrid materials constructed of inserted fiber polymer composites between thin layers of metal [1, 2]. Aluminum (Al) alloys are the prime materials employed in the manufacturing of FMLs, which are extensively used in the automobile and aircraft industries. Natural fibers have increasingly been employed as reinforcing materials in polymer composites in recent years because they are readily available, are inexpensive, provide excellent thermal and acoustic insulation, have remarkable mechanical properties, are renewable, and can be recycled [3, 4]. These profits make natural fibers an attractive alternative to synthetic fibers for a variety of uses, either entirely or partially. Despite their appeal, natural fibers have a few drawbacks over synthetic fibers, including a high degree of inconsistency, poor mechanical and moisture resistance, and reduced impact resistance. Due to its low cost, light weight, and availability, jute (J) is one of the most talented natural fibers [5–7]. J-fiber-based composites are a promising material for low load-bearing requests [8, 9].

By keeping the benefits of these fibers while reducing some of their drawbacks, hybrid composites are thought to give structures with a stable effect from the fibers used [10, 11]. Because they can be readily customized to provide greater characteristics that are impossible to achieve with a single fiber-reinforced composite, hybrid composites are becoming increasingly popular [12]. By combining weaker fibers with stronger fiber, hybridization can increase the stiffness, strength, and moisture resistance of composites, thus overcoming their drawbacks. As a result, the hybridization procedure may be used as a tactic to increase the use of various fiber-reinforced composites in a variety of applications [13, 14].

Many works in the literature discuss the mechanical properties of FMLs established on natural fibers [15–17]. Although many researchers have looked at FMLs made of natural fibers, as stated above, there have been fewer studies done on FMLs made of natural/synthetic hybrid fibers. The tensile, compression, and flexural properties of natural/synthesis fibers with metal laminates were studied by Mohammed et al. [18]; the materials used were flax (F) fibers, kenaf (K) fibers, carbon (C) fibers, aluminum (Al) alloy 2024 and epoxy. Two hybrid FMLs were made with different stacking orders of natural/synthesis. The laminates were made from (C) and (F) fiber-reinforced (Al) named (CAFRALL), while the laminates were made from (C) and (K) fiber-reinforced (Al) named (CAKRALL).

The experimental results revealed that CAKRALL had the highest elasticity modulus of 4.4 GPa and produced better tensile and compressive strength than CAFRALL with an improvement of 14.8 and 20.4%, respectively, while CAKRALL has 33.7% flexural strength lower than CAFRALL.

Zareei et al. [19] examined the tensile and interlaminar shear (ILSS) characteristics of eco-friendly fiber metal laminates (EFFMLs) with jute (J)–basalt (B) textiles as a hybrid reinforcement and Al 2024-T6 as a coating and an epoxy as a matrix component. Al/2 J/2B/2 J/Al and Al/2B/2 J/2B/Al are sandwiched constructions; also, Al/J/B/J/B/J/B/Al and Al/B/J/B/J/B/J/Al are intercalated constructions. The results showed that the jute and basalt fibers sandwiched between them had the highest tensile strength, elastic modulus, and interlaminar shear strength (ILSS). Microstructural examinations further revealed that the (B) fibers had a strong link with the (Al) plies, but the (J) fibers had a weak one. It was also found that the lack of diffusion resulted in empty spaces between the (J) fibrils and that these faults were the main cause of the deterioration in mechanical characteristics. Feng et al. [20] investigated the combination of K/glass (G) FMLs' tensile strength and tension–tension fatigue life. The findings show that the material's tensile strength is increased by the addition of G-fabric. When G-fabric is substituted for center-K-fabric, the greatest fatigue resistance is obtained. Abd El-baky et al. [21] investigate the influence of stacking sequences and relative fiber amounts on novel hybrid FMLs constructed on Al 1050 alloy and J/G fiber-reinforced epoxy composites. Results showed that hybridization may be able to enhance the tensile and flexural characteristics of FMLs made from jute fabric. When glass/epoxy laminas are substituted for some of the jute/epoxy laminate's partial laminas, the flexural strength of FMLs created from jute fabric is increased. It is understood that adding high strength fibers to a composite core results in a material with greater tensile properties but lower flexural resistance.

Based on the above-mentioned literature survey, it is clear that limited research has focused on the investigation of the mechanical properties of fiber metal laminates (FMLs) based on natural/synthetic fibers. So, the current work aims to study the mechanical properties of FMLs of natural/synthetic hybrid fibers by various mechanical tests such as tension, flexural, in-plane shear, interlaminar shear, and bearing. The designed FMLs were prepared by hand lay-up and compression casting methods. The metal used in the developed FMLs was aluminum alloy 1050 (AA 1050) with a thickness of 0.5 mm, and the fabrics used in the composite parts are jute (J), glass (G), aramid (A), carbon (C), and basalt (B). The impact of hybridizing other declared fabrics with jute reinforced composites on the mechanical response of the designed laminates was evaluated.

## 2 Methodology

### 2.1 Materials

In this work, aluminum alloy (AA 1050) in the form of sheets with 0.5 mm thickness was used as a skin layer in the designed FMLs. The chemical composition of AA 1050 is (Al: 99.5%, Cu: 0.05%, Fe: 0.4% , Mn: 0.05%, Mg: 0.05%, Si: 0.25%, Ti: 0.03%, V: 0.05%, Zn: 0.05%). AA 1050 is a popular grade of aluminum with high ductility, a highly reflective finish, excellent corrosion resistance, and moderate strength [22]. 2 × 2 twill weave carbon (C) and 0°/90° plain weave jute (J), E-glass (G), aramid (A), and basalt (B) fabrics with a constant areal density of 200 g/m<sup>2</sup> were used as reinforcements to manufacture the designed FMLs. Woven materials were chosen because they provide easy processing, balanced characteristics, and the highest level of resilience to plane shear [23]. The matrix material selected was Kemapoxy 150 RGL. It has two parts, resin and hardener. Kemapoxy 150 RGL is characterized by a

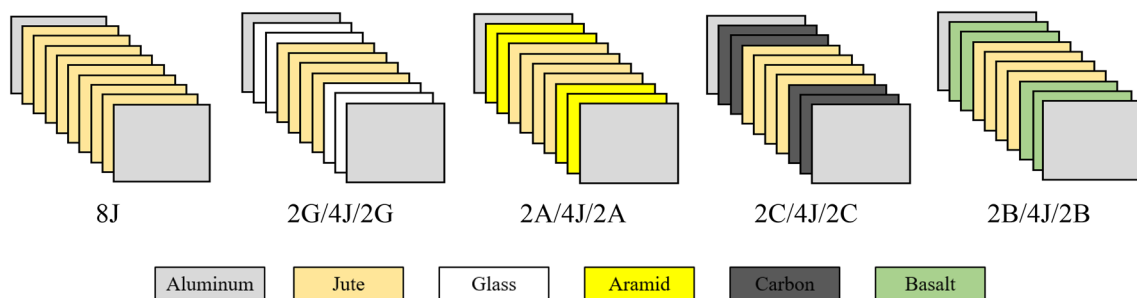
high resilience to chemical and mechanical stresses; it has been efficiently used in many works in the literature [14, 24, 25]. The properties that were provided by the producer for the used Al alloy, reinforcements, and epoxy are displayed in Table 1.

### 2.2 Fabrication of FMLs

The intended FMLs were created using hand lay-up and compression casting; the hand layup procedure was adapted by many authors because of its ease and low cost [26–30]. According to the designed sequences, as shown in Fig. 1, and mentioned in detail in Table 2 for more illustrations. Al-sheets underwent mechanical and chemical treatments to guarantee proper adhesion between Al-sheets and polymer composites. Al-sheets were exposed to a mechanical procedure that involved rinsing them in acetone, roughening them smoothly with # 400 grit sandpaper, see Fig. 2a, then rinsing them in tap water, see Fig. 2b, and drying them in an oven. To increase the Al-surface roughness, hydrochloric acid (HCl) was applied chemically to the mechanically treated

**Table 1** Mechanical properties of Al alloy, reinforcements and epoxy given by the producers

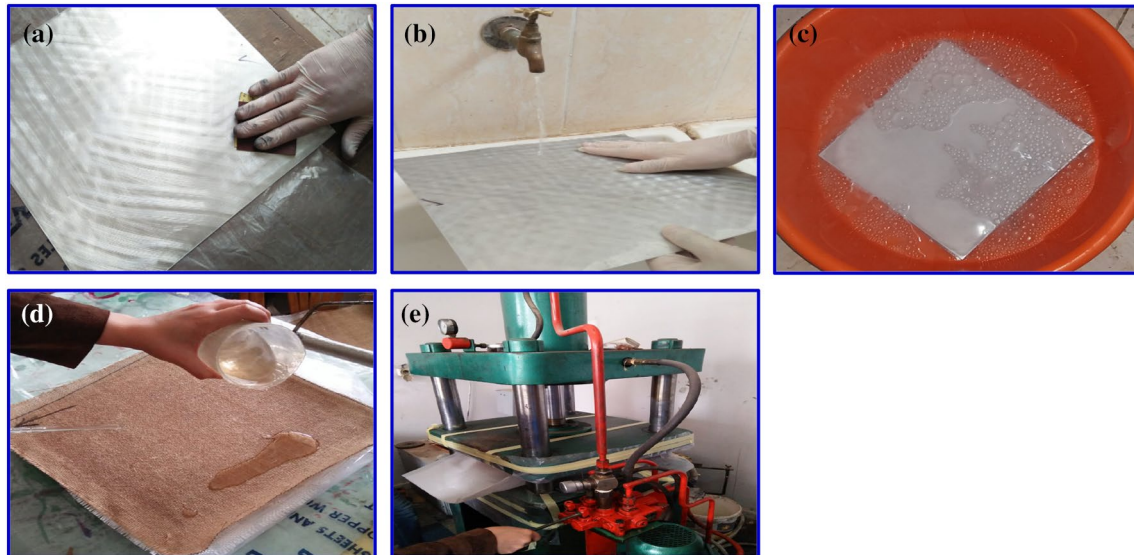
Material	Producer	Density (g/cm <sup>3</sup> )	Young's modulus (GPa)	Tensile strength (MPa)	Elongation (%)	Poisson's ratio
Al 1050	Metallurgical Industries Co. Ltd. Egypt	2.71	71	100	12	0.33
Jute (J)	Hangzhou Zhong Xing Cotton and Jute Co. Ltd. China	1.35	17	470	1.5–1.8	0.38
E-glass (G)	Hebei Yuniu Fiber Glass Manufacturing Co. Ltd. China	2.50	76	3400	1.8–3.2	0.22
Aramid(A)	Yixing Zhongfu Carbon Fiber Products Co., Ltd. China	1.40	67	3000:3150	2.5:3.6	0.36
Carbon (C)	Yixing Yitai carbon fiber weaving Co. Ltd. China	1.90	260	4200:4800	1.75–1.95	0.279
Basalt (B)	Quanzhou Basalt Manufacturing Co. Ltd. China	2.80	79	3000–4840	3.15	0.2
Kemapoxy 150 RGL	Chemicals for Modern Buildings Co. Ltd. Egypt	1.1	1.2	55:58	2.2:2.9	0.35



**Fig. 1** The sequences order for the designed FMLs

**Table 2** Description of the designed FMLs

Sequences order code	Description
8J	8 layers of jute fabrics sandwiched between two (AA 1050) sheets
2G/4J/2G	2 layers of glass fabrics, 4 layers of jute fabrics, and 2 layers of glass fabrics sandwiched between two (AA 1050) sheets
2A/4J/2A	2 layers of aramid fabrics, 4 layers of jute fabrics, and 2 layers of aramid fabrics sandwiched between two (AA 1050) sheets
2C/4J/2C	2 layers of carbon fabrics, 4 layers of jute fabrics, and 2 layers of carbon fabrics sandwiched between two (AA 1050) sheets
2B/4J/2B	2 layers of basalt fabrics, 4 layers of jute fabrics, and 2 layers of basalt fabrics sandwiched between two (AA 1050) sheets

**Fig. 2** The fabrication process for the designed FMLs

sheets at a volumetric proportion of 11%. For 30 min, acid etching was done at room temperature. Following a water rinse, all linens were dried. Al-sheets were then submerged for 5 min at 70 °C in a 5-weight percent NaOH solution, see Fig. 2c. After being washed with tap water to eliminate the remaining oxide, the oxidized Al-sheets were dried in an oven to stabilize the oxide coating [22, 28, 31]. The treated Al-sheets and woven fabric layers were covered with a uniform layer of the mixture (epoxy and its hardener), see Fig. 2d. For 24 h at room temperature, the constructed laminates were kept under 2.5 bars of pressure to cure, as shown in Fig. 2e. After 21 days, mechanical tests were conducted to ensure maximum strength and a full recovery. No residual stress is produced in the manufactured laminates because the cure procedure was carried out at room temperature [32, 33].

### 2.3 Mechanical Testing

Tensile, flexural, in-plane shear, interlaminar shear, and bearing tests on the proposed FMLs were carried out on

the universal testing machine (UTM) (type: Jinan WDW, China (Mainland), 100 kN) at a strain rate of 2 mm/min at room temperature. To ensure consistency, three identical samples for each FML were examined. The average result was recorded.

#### 2.3.1 Tensile Test

A basic test in material science is the tensile test, which involves applying a controlled tensile force to the tested specimen until failure. The manufacturing laminates were cut into strips measuring 250 × 25 mm<sup>2</sup>, as prescribed by ASTM D3039. Each test specimen's gripping area was epoxy-glued to four rectangular aluminum tabs. These tabs, which help distribute pressure from the machine to the specimen and lessen stress concentration from the grips, protect the specimen from crushing between the testing equipment's grips. [34, 35]. Stress–strain curves were created for each sample using the testing data. The ultimate tensile strength ( $\sigma_{ult}$ ), the apparent tensile modulus ( $E_{app}$ ) and the toughness

modulus ( $U_T$ ) were all assessed using the relations presented below:

$$\sigma_{ult} = \frac{P_{max}}{bh} \tag{1}$$

$$E_{app} = \frac{\Delta\sigma_t}{\Delta\varepsilon_L} \tag{2}$$

$$U_T = \frac{\text{Energy}}{\text{Volume}} = \int_0^{\varepsilon_f} \sigma d\varepsilon \tag{3}$$

where  $P_{max}$  is the maximum applied load,  $\Delta\sigma_t/\Delta\varepsilon_L$  means the stress–strain curve's initial linear segment's slope, and  $\varepsilon_f$  signifies the failure strain.  $b$  and  $h$  are the specimen's measured width and thickness, respectively.

### 2.3.2 Flexural Test

The flexural properties of the manufactured FMLs in accordance with JIS K7055 were assessed using a three-point flexural test. Considering the test results recorded, the flexural strength ( $\sigma_{fl}$ ), flexural strain ( $\varepsilon_{fl}$ ), and flexural modulus ( $E_{fl}$ ) were estimated according to the following equations:

$$\sigma_{fl} = \frac{3P_{max}L}{2bh^2} \tag{4}$$

$$\varepsilon_{fl} = \frac{6\delta h}{L^2} \tag{5}$$

$$E_{fl} = \frac{L^3 m}{4bh^3} \tag{6}$$

where  $L$  is the span length which is 80mm,  $\delta$  is the exciting bend of the midpoint, and  $m$  is the load-deformation plot's straight line's slope ( $m = \Delta P/\Delta\delta$ ).

### 2.3.3 In-Plane Shear Test (the [45]<sub>±ns</sub> Laminate Tensile Test)

An easy way to determine the unidirectional lamina's in-plane shear characteristics is to perform the [45]<sub>±ns</sub> laminate tensile test. The test specimen is relatively easy to prepare, and normal tensile grips are all that are needed as test fixtures. As per ASTM D3518, the testing procedure has been standardized. This test method's greatest advantage is the ease with which it is prepared and conducted. However, this shear test suffers from a combination of a biaxial tensile stress state and shear stress. Each lamina contains normal tensile stresses  $\sigma_1$  and  $\sigma_2$ , in addition to the desired shear stress  $\tau_{12}$ . Furthermore, the interlaminar shear stress  $\tau_{xz}$  presents near the lamina free edge. According to biaxial failure theories, shear and in-plane stress components interact to

determine failure. The determination of the shear stress and shear strain in the principle planes of the  $\pm 45^\circ$  plies is based on a stress analysis of the [45]<sub>ns±</sub> specimen. The in-plane shear stress can be simply calculated as follows:

$$\tau_{12} = \frac{P}{2A} = \frac{\sigma_x}{2} \tag{7}$$

where  $P$ ,  $A$  and  $\sigma_x$  are the applied load, the average cross-sectional area and the average axial stress, respectively.

### 2.3.4 Interlaminar Shear Test

The apparent interlaminar shear strength (ILSS) of the manufactured FMLs was measured using the short beam shear (SBS) test in accordance with ASTM D 2344. A 4.5 span-to-thickness ratio and a 6.0 length-to-thickness ratio are required by the law. Each specimen had two lateral-moving roller supports that were loaded at the center of each specimen. The specimen was loaded up to the point of failure, and the failure load served as a measurement of the apparent ILSS. The apparent ILSS can be calculated as follows:

$$\text{ILSS} = \frac{0.75P_{max}}{bh} \tag{8}$$

### 2.3.5 Bearing Test

A bearing test was performed according to ASTM D5961/D5961M, and test specimens were made into strips measuring  $130 \times 36 \text{ mm}^2$ . Net tension, shear-out, and bearing are the three primary failure mechanisms that can be identified in a pin-loaded specimen during a bearing test. Mixing of various modes can also be categorized using the geometric characteristics of the joint, such as the edge distance-to-hole diameter ratio ( $e/d$ ) and width-to-hole diameter ratio ( $w/d$ ). In this investigation, it was discovered that ( $e/d$ ) and ( $w/d$ ) were, respectively, 3 and 6. The bearing strength ( $\sigma_b$ ) was considered as follows:

$$\sigma_b = \frac{P_{max}}{dt} \tag{9}$$

## 3 Results and Discussion

### 3.1 Tensile Properties

A comparison plot of the stress–strain curves for the tested FML specimens is shown in Fig. 3. As seen in Fig. 3, the stress–strain curve for each specimen displays a linear tendency up to the maximum force. After that, a sharp failure was noted. Figure 4 shows the obtained mechanical

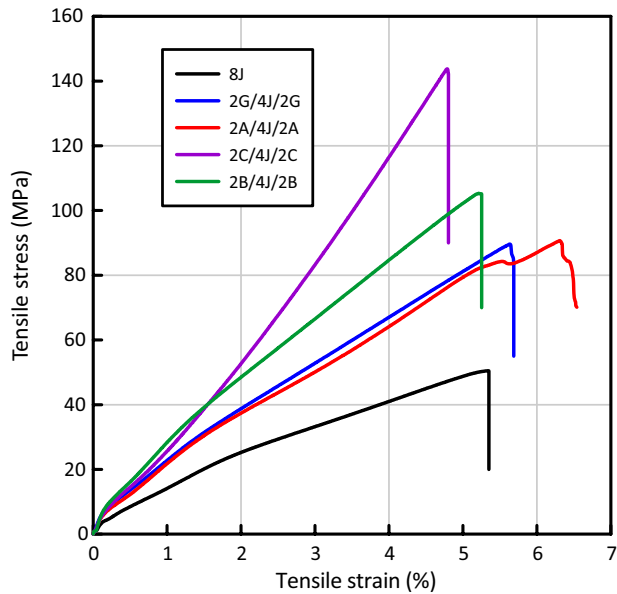


**Fig. 3** Tensile stress–strain curves for the tested FMLs (obtained from the testing machine)

properties of studied FMLs. Consequently, as shown in Fig. 4a, that 2C/4J/2C specimen presents the highest ultimate tensile strength with a value of 137.29 MPa with an improvement of 181.9% over the 8 J specimen which records the lowermost ultimate tensile strength of 48.7 MPa. Also, there is an improvement of 89.67, 92.46, and 114% for, respectively, 2G/4J/2G, 2A/4J/2A, and 2B/4J/2B. A similar result was recorded by Malingam et al. [36] for hybrid FMLs based on K- and G-fibers. Zareei et al. [19] for FMLs consisted of J-layers sandwiched by B-layers and Abd El-baky et al. [21] for FMLs consisted of J-layers sandwiched by G-layers.

Figure 4b states the tensile failure strain of the designed FMLs. The highest and lowest failure strain values were observed for 2A/4J/2A and 2C/4J/2C specimens with values of 6.37 and 4.59%, respectively. Also, it can be noted that the tensile failure strain compared with the 8J specimen increased by 13.74, 21.56, and 1.9% for 2G/4J/2G, 2A/4J/2A, and 2B/4J/2B, respectively, while decreasing by 12.40% compared with the 2C/4J/2C specimen. It is clear that hybridization of jute with glass, aramid, carbon, and basalt fabrics significantly influences the tensile failure strain. The tensile toughness modulus of the manufactured FMLs is shown in Fig. 4c. With values of 3.40 and 1.57 MPa, respectively, the 2A/4J/2A and 8J specimens showed the greatest and lowest toughness modulus values. It is also important to observe that for the 2G/4J/2G, 2A/4J/2A, 2C/4J/2C, and 2B/4J/2B specimens, the toughness modulus increased by 80.25, 116.56, 107, and 96.18%, respectively.

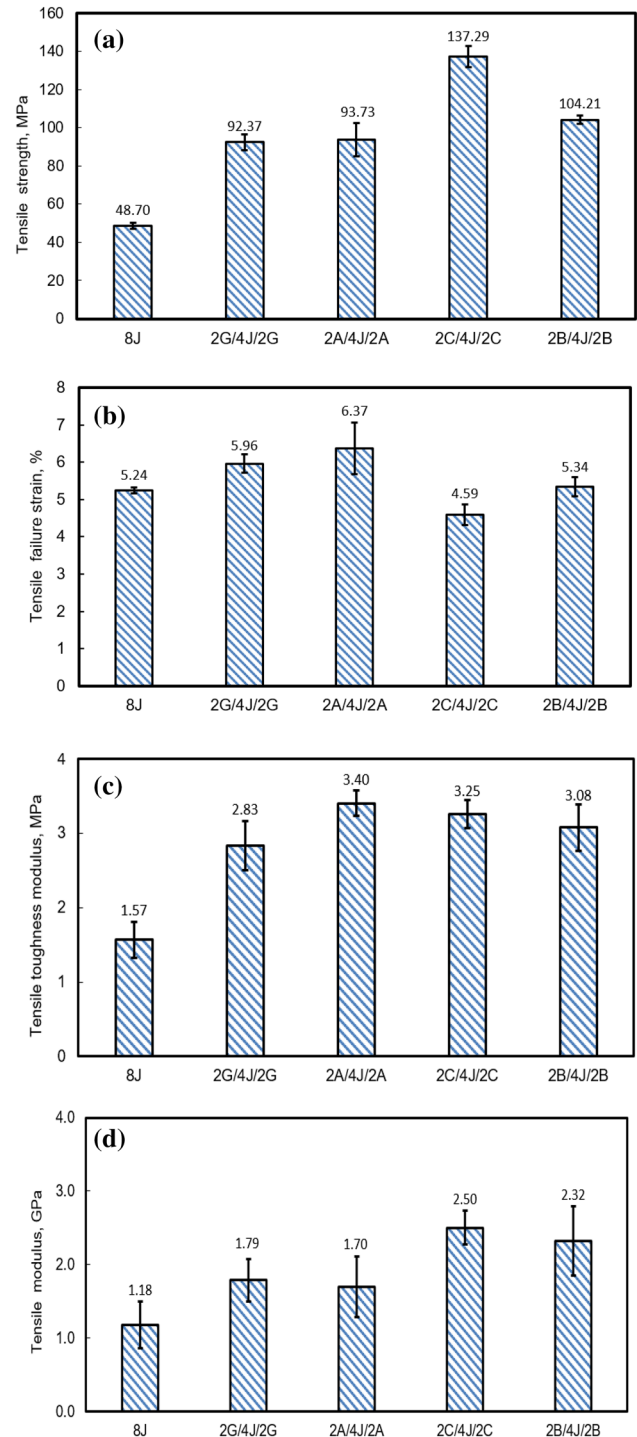


**Fig. 4** **a** Ultimate tensile strength, **b** failure strain, **c** toughness modulus for the tested FMLs, and **d** apparent tensile modulus

Regarding the apparent modulus of elasticity, it is clear from Fig. 4d that the apparent modulus of elasticity increased by 51.69, 44.10, 111.86, and 96.61% for the 2G/4J/2G, 2A/4J/2A, 2C/4J/2C, and 2B/4J/2B specimens, respectively.

Figure 5 displays the failure signs of tensile test specimens; severe debonding between composite and Al layers due to bad bond was observed for 8J, 2G/4J/2G, 2C/4J/2C, and 2B/4J/2B, as shown in the representative samples displayed in Fig. 5a. Whilst a good bond was seen between composite components, a similar result was documented by Zareei et al. [19] for FMLs reinforced by hybrid B- and J-fabrics. In addition to debonding between composite parts and Al layers, debonding between composite constituents was also detected for the 2A/4J/2A specimen, as shown in Fig. 5b.

### 3.2 Flexural Properties

The flexural strength, modulus, and strain for the tested FMLs are exhibited in Fig. 6. As shown in Fig. 6a, the maximum and minimum flexural strengths were observed for 2G/4J/2G and 2A/4J/2A with values of 78.30 and 45.27 MPa, respectively. It is also clear that hybridization improves the flexural strength of 8 J specimen by 51.51, 35.39, and 41.25%, respectively, for 2G/4J/2G, 2C/4J/2C, and 2B/4J/2B, but decreases it by 12.4% compared with the 2A/4J/2A specimen. The flexural strain for the tested FMLs is shown in Fig. 6b. It is obvious that the 2C/4J/2C and 2A/4J/2A specimens have values of 18.84 and 11.19%, respectively. It is also evident that hybridization reduced 8J sample for 2A/4J/2A and 2B/4J/2B by 28 and 9.10%, respectively, but improved them for 2G/4J/2G and 2C/4J/2C by 3.28 and 21.24%. Similar results were recorded by Rajkumar et al. [37] for hybrid FMLs based on G-fiber and C-fiber. Regarding the flexural modulus, Fig. 6c clearly shows that the 2G/4J/2G and 8J specimens with values of 13.43 and 4.30 GPa, respectively, had the greatest and lowest flexural modulus values. Additionally, for 2G/4J/2G, 2A/4J/2A, 2C/4J/2C, and 2B/4J/2B, respectively, hybridization improves the 8J specimen by 212.33, 173.95, 155.58, and 198.60%.

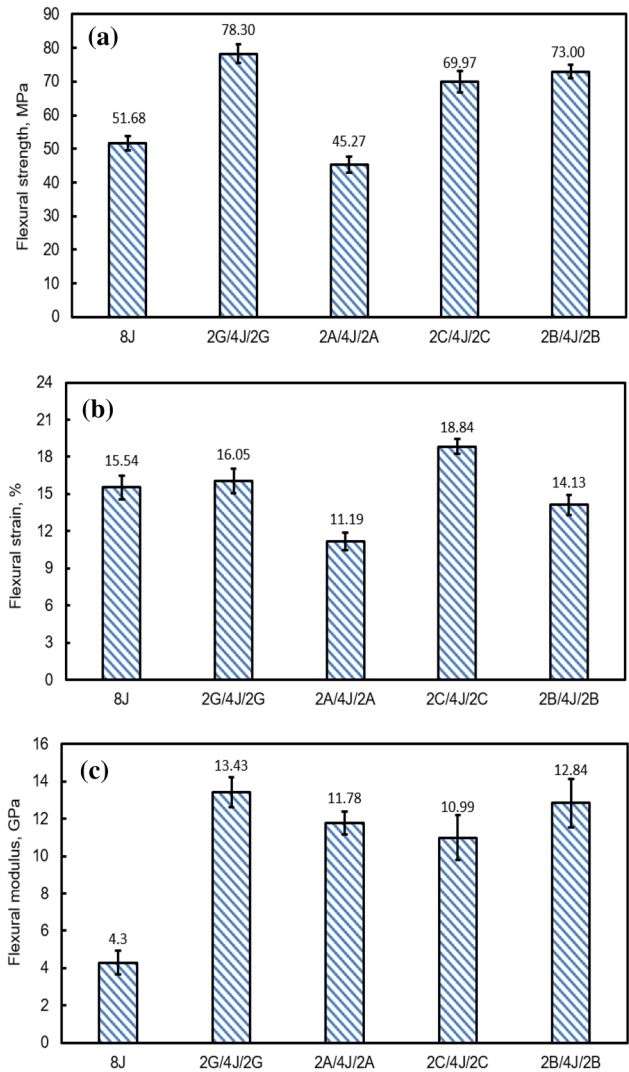


Fig. 6 Flexural a strength, b strain, and c modulus for the tested FMLs

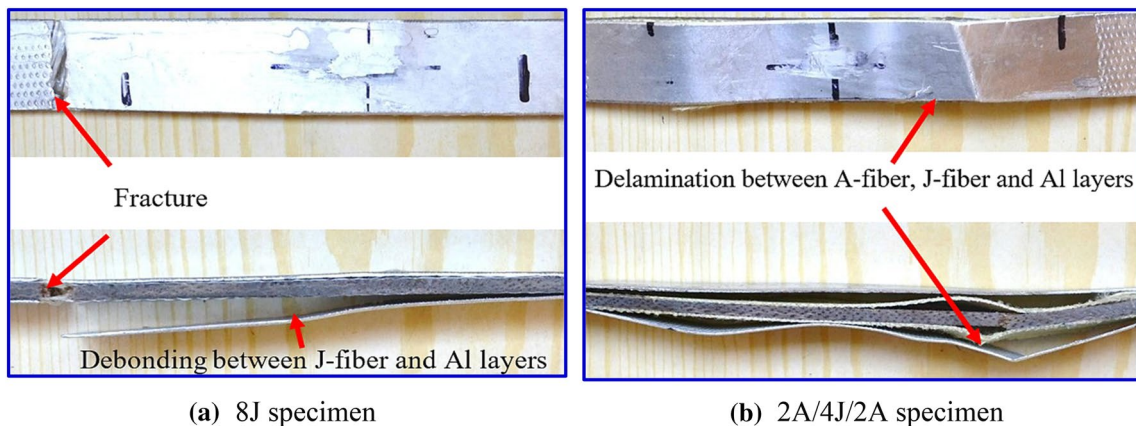


Fig. 5 Failure signs for the tested FMLs under tensile load

The failure signs of the tensile test specimens are shown in Fig. 7, where extreme debonding between the composite and Al layers because of a poor bond was seen for the specimens 8J, 2G/4J/2G, 2C/4J/2C, and 2B/4J/2B, as shown in the symbolic sample exhibitions in Fig. 7a. While an intense bond was observed between the composite parts, the same results were obtained by Alshahrani et al. [6] between jute–basalt reinforced epoxy hybrid composites. Debonding between the components of the composite, as well as between the composite part and the Al layers, was found in the 2A/4J/2A specimen, as depicted in Fig. 7b. This is consistent with that recorded by Li et al. [38] and Hynes et al. [39].

### 3.3 In-Plane Shear Properties

The in-plane shear strength of the fabricated FMLs is shown in Fig. 8. It is clear that, with a value of 20.65 MPa, the 2C/4J/2C specimen had the maximum in-plane strength, while the 2A/4J/2A specimen had the lowest value of 15.00 MPa. The in-plane shear strength of jute fabric improved by 20.38, 26.38, and 11.20% for 2G/4J/2G, 2C/4J/2C, and 2B/4J/2B, respectively, when the fabric was hybridized with glass, carbon, and basalt. On the other hand, jute fabric hybridization decreased the in-plane shear strength by 8.20% for a 2A/4J/2A specimen.

The failure signs of the in-plane shear test specimens are presented in Fig. 9. Severe debonding between the composite and Al layers as a result of a poor bond was seen for the specimens 8J, 2G/4J/2G, 2C/4J/2C, and 2B/4J/2B, as displayed in the example samples in Fig. 9a. While a strong connection was observed between composite parts, matching

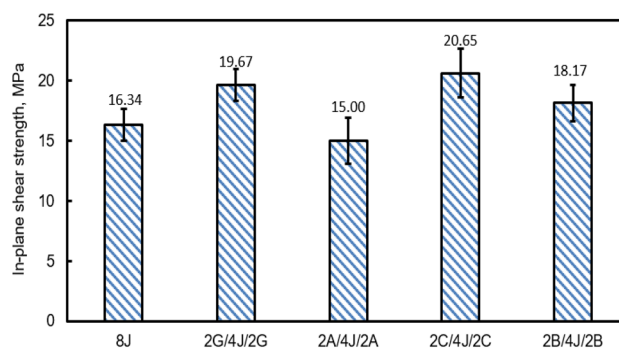


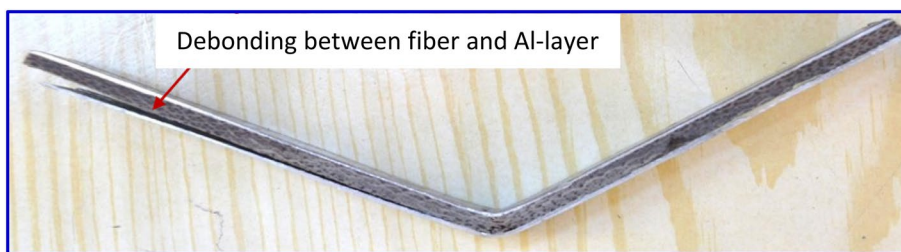
Fig. 8 In-plane shear strength of tested FMLs

outcomes were found by Alshahrani et al. [6] between J-B-reinforced epoxy hybrid composites. Debonding between the components of the composite, as well as between the composite part and the Al layers, was found in the 2A/4J/2A specimen, as depicted in Fig. 9b.

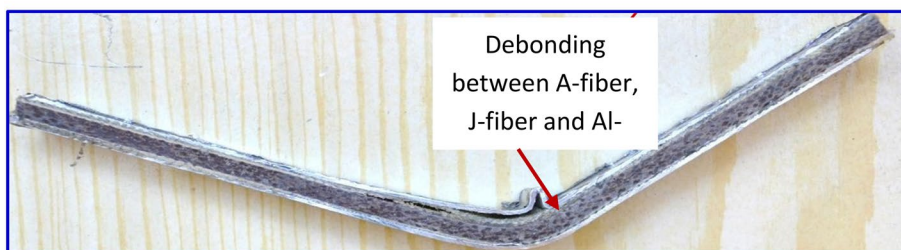
### 3.4 Interlaminar Shear Strength (ILSS)

Figure 10 shows the manufactured FMLs' ILS strength. It is evident that the 2G/4J/2G specimen had the highest ILS strength, measuring 4.71 MPa, followed by the 8J specimen at 4.07 MPa, and the 2C/4J/2C specimen had the lowest number, 2.94 MPa. The hybridization of jute fabric with aramid, carbon, and basalt had a detrimental impact on ILS strength, as ILS strength dropped by 14.74, 27.76, and 9.10% for 2A/4J/2A, 2C/4J/2C, and 2B/4J/2B, respectively. On the other hand, for a 2G/4J/2G specimen, hybridization J-fabric with glass-fabric increases ILS strength by 15.72%.

Fig. 7 Failure signs for the tested FMLs under flexural load



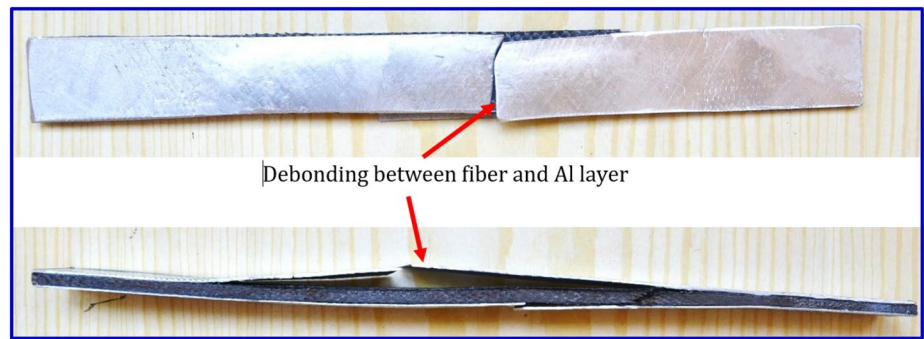
(a) 8J specimen



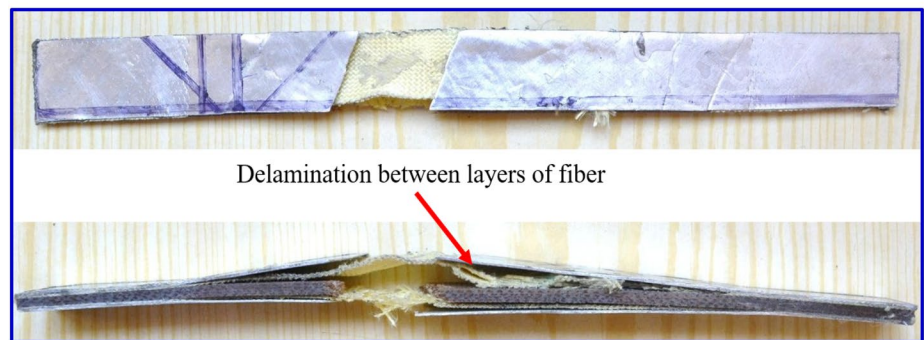
(b) 2A/4J/2A specimen



**Fig. 9** Failure signs for the tested FMLs under in-plane shear load



(a) 2G/4J/2G specimen



(b) 2A/4J/2A specimen

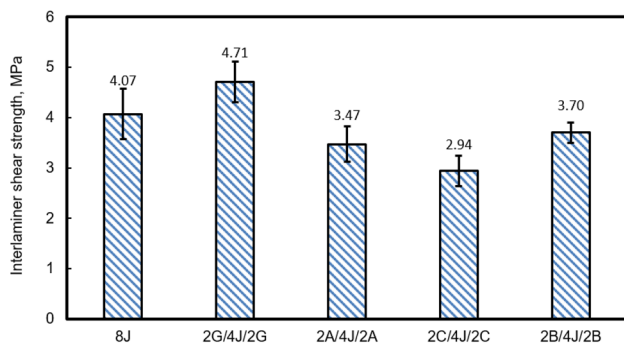
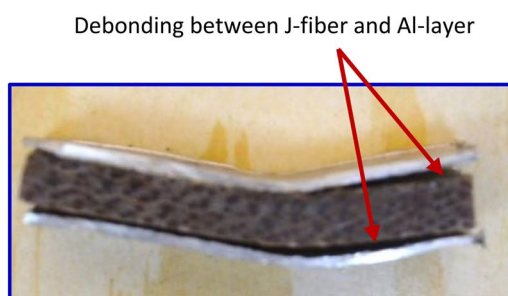
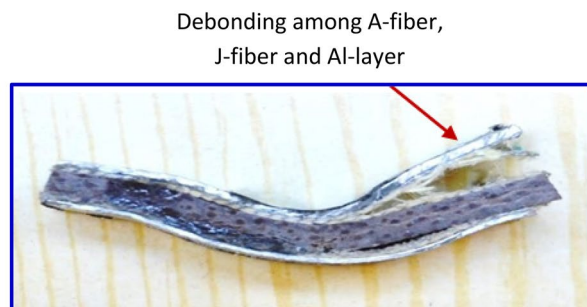


**Fig. 10** Interlaminar shear strength of tested FMLs

Delamination is a significant failure mechanism caused by interlaminar shear stress. Localized damage to material under the loading nose constitutes a failure. The bending moment causes a tensile force to be created at the specimen's bottom. This stress is weighty enough to cause delamination. A severe deboning between the composite and Al layers as a result of a weak bond was seen for the test specimens 8J, 2G/4J/2G, 2C/4J/2C, and 2B/4J/2B, as shown in the typical samples displayed in Fig. 11a. While a strong connection was observed between composite parts, Zareei et al. [19] documented a similar outcome for FMLs reinforced with hybrid B-fabric and J-fabric. Deboning between the



(a) 8J specimen



(b) 2A/4J/2A specimen

**Fig. 11** Failure signs for the tested FMLs under interlaminar shear load

components of the composite, as well as between the composite portion and the Al layers, was found in the 2A/4J/2A specimen, as depicted in Fig. 11b. This agrees with what was recorded by Hu et al.[40].

### 3.5 Bearing Properties

The bearing strength of the proposed FMLs is exposed in Fig. 12. It is clear that the maximum bearing strength was observed for the 2C/4J/2C specimen with a value of 322.19 MPa followed by the 2B/4J/2B specimen with a value of 296.99 MPa, whilst the minimum value was recorded for the 2G/4J/2G of 186.45 MPa. A negative effect on bearing strength was noted with the hybridization of jute fabric with glass and aramid as bearing strength decreased by 6.86 and 4.18%, respectively, for 2G/4J/2G and 2A/4J/2A. On the contrary, hybridization of jute fabric with carbon and basalt improves bearing strength by 60.94 and 48.35 for 2C/4J/2C and 2B/4J/2B, respectively.

For the tested FMLs during the tension bearing test, a mixed bearing/net tension failure mode was found, as shown in Fig. 13. Broad white areas caused by delamination and a broad failure area on the pin/hole contact area are characteristics of the bearing failure region. Net tension rupture occurred in 8J specimens, as shown in Fig. 13a. It is categorized using local fiber–matrix debonding, net-tension fractures, layer detachments, and fiber weakening. These events are caused by the matrix weakening, the fiber–matrix link

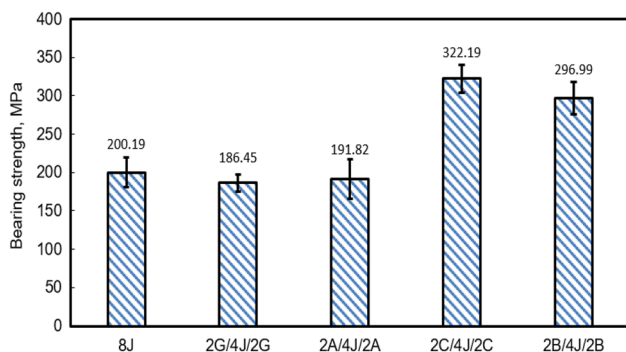


Fig. 12 Bearing strength of tested FMLs

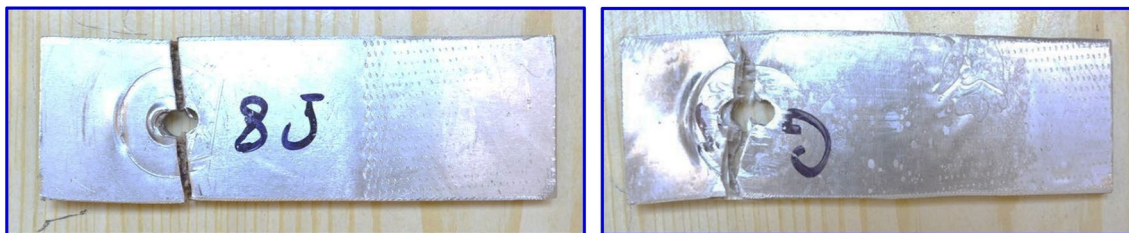


Fig. 13 Failure signs for the tested FMLs under bearing load

deteriorating, and the natural fibers' decreasing mechanical characteristics. These concentrated damages can be linked to the beginning of joint-damaging events brought on by the shear out mode, which interacts with the net-tension mode to reduce joint mechanical strength. In addition to the net-tension fracture, the area between the hole and the free edge shows a notable surface whitening caused by laminae debonding as a result of bearing failure. Nonlinear deformation curves are the outcome of this gradual damage occurrence; this mode was detected for 2G/4J/2G, 2C/4J/2C, 2A/4J/2A, and 2B/4J/2B, as shown in the representative sample shown in Fig. 13b.

### 3.6 Microstructural Examination

Damage in polymer composites is influenced by several factors, including fiber type, orientation, volume percentage, matrix type, lay-up order, and fiber–matrix interfacial bonding. In order to understand the failure of the hybrids under various stress scenarios, the fracture surfaces of the specimens were examined using SEM JSM 6100. The fracture location was treated with gold, which was then kept in an ionizer. To take pictures, a voltage of 20 kV was applied to the surfaces. All microscope pictures were taken through the laminate's thickness after the tension tests. SEM pictures of the failed surfaces of tensile specimens are shown in Fig. 14. There were apparent signs of, fiber ripping out, delamination, and cracking. Surface cracks could be seen on all test specimens, which eventually caused specimen cracking.

## 4 Future Work and Recommended Applications

The current research can be expanded to look into additional critical FML-related issues. The topics listed below are some suggestions for upcoming works:

- Studying the effects of the hybridization procedure on the dynamic properties through impact tests at low and high velocities.
- Investigating the fatigue behavior of the designed FMLs.

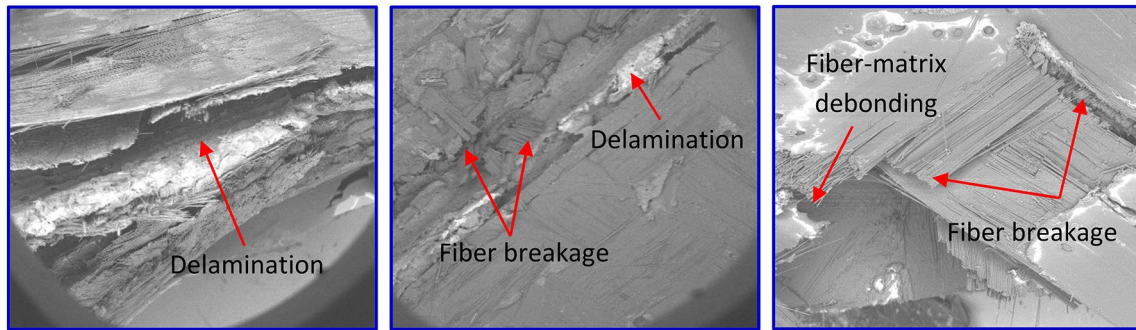


Fig. 14 SEM of the designed FMLs under tensile loading

- Exploring the influence of other types of natural fibers and other stacking orders.
- Determining the effect of environmental factors such as heat and moisture.
- It is suggested to do a numerical model to decrease costs and expedite the understanding of the structure’s response.

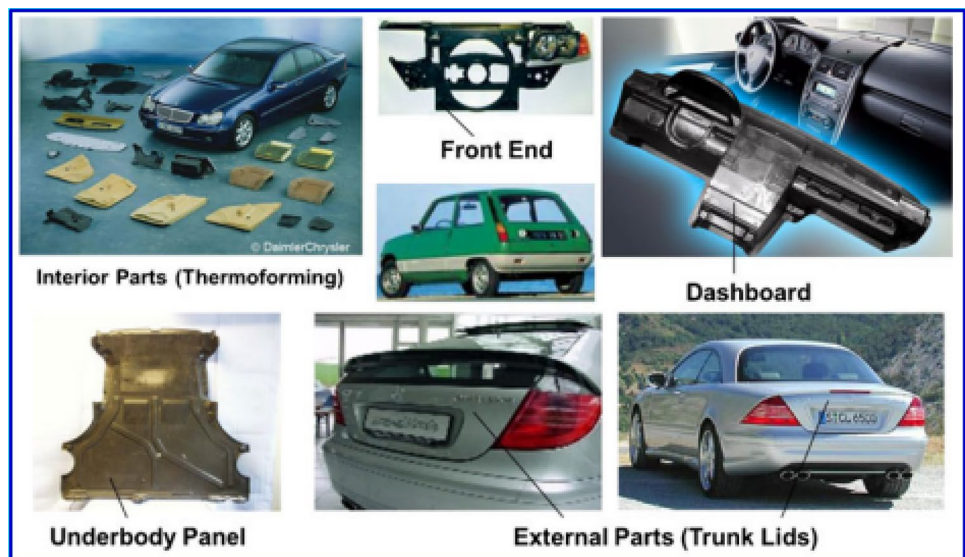
Numerous automotive parts, such as longitudinal fronts, floors, roofs, firewalls, rear walls, side panels, under body panels, dashboard elements, door trim panels, seat cushions, real panel shelves, car frames, dashboard designs, headliners, decking, pallets, and headliners, can be fitted with the suggested FMLs, as shown in Fig. 15.

### 5 Conclusions

The present work aims to investigate experimentally the influence of hybridization between jute-reinforced composite and other specified fabrics on the mechanical characteristics of fiber metal laminates (FMLs). The designed laminates were created for this purpose using aluminum sheets and various types of fabric, including jute (J), glass (G), aramid (A), carbon (C), and basalt (B). The constructed laminates were subjected to a variety of mechanical tests, including tensile, flexural, in-plane shear, interlaminar shear, and bearing tests. The preparation of the specimens used hand lay-up and compression casting techniques. The next conclusions were reached:

- The hybridization was found to have weighty influences on the mechanical properties of the designed FMLs.
- The tensile factors of the 2G/4J/2G [AA1050/2 glass layers/4 jute layers/2 glass layers/AA 1050] specimen,

Fig. 15 Recommended applications of FMLs in vehicles



including its ultimate tensile strength, strain to failure, toughness modulus, and apparent tensile modulus, are improved by the addition of glass fabric. Additionally, they increase the flexural strain, flexural strength, and flexural modulus, enhancing the interlaminar and in-plane shear strengths as well. Hybridization has a negative impact on bearing strength in terms of bearing strength.

- The 2A/4J/2A [AA1050/2 aramid layers/4 jute layers/2 aramid layers/AA 1050] specimen, which combines aramid fabric and jute reinforcement, increase the tensile properties of the material, including ultimate tensile strength, tensile strain to failure, tensile toughness modulus, and apparent tensile modulus, and enhance the flexural modulus while lowering the flexural strength and strain. Both the in-plane and interlaminar shear strength, and the bearing strength were reduced by hybridization.
- The tensile properties of 2C/4J/2C [AA1050/2 carbon layers/4 jute layers/2 carbon layers/ AA 1050] specimens are improved by the addition of carbon fabric. These improvements include improved ultimate tensile strength, tensile toughness modulus, and apparent tensile modulus, but reduced tensile failure strain. Additionally, they increase the flexural tension, flexural strength, and flexural modulus. Furthermore, it improved the in-plane shear strength, whilst decreasing the interlaminar shear strength. Hybridization significantly increases bearing strength with respect to bearing properties.
- The materials, i.e., the designed FMLs' tensile properties, such as ultimate tensile strength, tensile strain to failure, tensile toughness modulus, and apparent tensile modulus, are improved in the 2B/4J/2B [AA1050/2 basalt layers/4 jute layers/2 basalt layers/AA 1050] specimen, which combines basalt fabric and jute reinforcement, reducing flexural tension while increasing flexural strength and modulus. Concerning the shear properties, hybridization increased the in-plane shear strength, but reduced the interlaminar shear strength. Regarding bearing characteristics, hybridization increases bearing strength.

**Acknowledgements** The author would like to thank Prince Sultan University for their support. The authors are thankful to the Deanship of Scientific Research at Najran University for funding this work, under the Research Groups Funding program grant code (NU/RG/SERC/12/8).

**Author Contributions** MMAA did writing the original copy, drawing the curves, analysis of data results, and preparing the final revision. DAH was involved in preparing the response to the reviewer's comments, revising the English quality, and preparing the final revision. HA prepared the response to the reviewer's comments and the final revision. TAS prepared the response to the reviewer's comments, revised the English quality, and prepared the final revision. MAAE

contributed to idea, experimental work, analysis of data results, supervision, preparing the final revision.

**Funding** This study was funded by Najran University, NU/RG/SERC/12/8, Hassan Alshahrani.

**Data availability statement** The datasets generated during and/or analyzed during the current study are available from the corresponding author on reasonable request.

## Declarations

**Conflict of interest** The author declares that there is no conflict of interests regarding the publication of this paper.

## References

1. X. Li, X. Zhang, Y. Guo, V.P.W. Shim, J. Yang, G.B. Chai, *Int. J. Impac. Eng.* **114**, 32 (2018)
2. M. Megahed, M.A. Abd El-baky, A.M. Alsaedy, A.E. Alshorbagy, *Compos. Pt B: Eng.*, **176**, 107277 (2019)
3. M.R. Sanjay, P. Madhu, M. Jawaid, P. Sentharamaikannan, S. Senthil, S. Pradeep, *J. Cleaner Prod.* **172**, 566 (2018)
4. N. Karthi, K. Kumaresan, S. Sathish, S. Gokulkumar, L. Prabhu, N. Vigneshkumar, *Mater. Tod. Proceed.* **27**, 2828 (2020)
5. D. Gon, K. Das, P. Paul, S. Maity, *Int. J. Text. Sci.* **1**, 84 (2013)
6. H. Alshahrani, T. A. Sebaey, M. M. Awd Allah, and M. A. Abd El-baky, *J. Compos. Mater.* (2023)
7. V. Mishra, S. Biswas, *Proced. Eng.* **51**, 561 (2013)
8. K.S. Ahmed, S. Vijayarangan, *J. Appl. Polym. Sci.* **104**, 2650 (2007)
9. A. Mache, A. Deb, N. Gupta, *Polym. Compos.* **41**, 1796 (2019)
10. P. Amuthakkannan, V. Manikandan, M. Uthayakumar, *J. Advanc. Microsc. Res.* **9**, 44 (2014)
11. V. Ganesan, B. Kaliyamoorthy, *J. Nat. Fib.* **19**, 1990 (2020)
12. S.I. Mavani, N.M. Mehta, P.H. Parsania, *J. Appl. Polym. Sci.* **106**, 1228 (2007)
13. M.A. Attia, M.A. Abd El-Baky, M.A. Hassan, T.A. Sebaey, E. Mahdi, *Poly. Compos.*, **39**, E2245 (2018)
14. M.A.A. El-baky, M.M.A. Allah, M. Kamel, W. Abdel-Aziem, *Fib. Polym.* (2023)
15. R.E. Farsani, S.M.R. Khalili, V. Daghigh, *Int. J. Damag. Mech.* **23**, 729 (2013)
16. D. Gunwant, *Int. J. Res. Appl. Sci. Eng. Tech.* **6**, 1391 (2018)
17. N.M. Ishak, D. Sivakumar, M.R. Mansor, *J. Brazil. Soc. Mech. Sci. Eng.* **40** (2018)
18. I. Mohammed, A.A. Talib, M.T.H. Sultan, M. Jawaid, A.H. Arifin, S. Saadon, *Bio. Res.* **13**, 2022–2034 (2018)
19. N. Zareei, A. Geranmayeh, R. Eslami-Farsani, *Polym. Test.* **75**, 205 (2019)
20. N.L. Feng, S. DharMalingam, K.A. Zakaria, M.Z. Selamat, *J. Sand. Struct. Mater.* **21**, 2440 (2017)
21. M.A. Abd El-Baky, A.E. Alshorbagy, A.M. Alsaedy, M. Megahed, *J. Nat. Fib.*, **19**, 303 (2020)
22. M. A. Abd El-baky and M. A. Attia, *Polym. Compos.*, **41**, 4130 (2020)
23. Z. Boufaïda, L. Farge, S. André, Y. Meshaka, *Compos. Pt A Appl. Sci. Manufact.* **75**, 28 (2015)
24. M. Megahed, D.E. Tobbala, M.A.A. El-baky, *Polym. Compos.* **42**, 271 (2020)
25. M.A.A. El-Baky, M.M.A. Allah, M. Kamel, W. Abd-Elaziem, *Sci. Rep.* **12**, 21101 (2022)

26. M.I.A. El Aal, M.M. Awd Allah, M.A. Abd El-baky, *Polym. Compos.*, (2023)
27. M.M. Awd Allah, A. Shaker, M.A. Hassan, M.A. Abd El-baky, *Polym. Compos.* (2022)
28. H. Alshahrani, T.A. Sebaey, M.M. Awd Allah, M.A. Abd El-baky, *Polym. Compos.* (2022)
29. H. Alshahrani, T.A. Sebaey, M.M. Awd Allah, M.A. Abd El-baky, *J. Compos. Mater.*, **57**, 1579 (2023)
30. H. Alshahrani, T.A. Sebaey, M.M. Awd Allah, M.A. Abd El-baky, *J. Compos. Mater.* (2022)
31. M.A.A. El-Baky, M.M.A. Allah, M. Kamel, W. Abd-Elaziem, *Sci. Rep.* **12**, 21097 (2022)
32. M. Megahed, M.A. Abd El-baky, A.M. Alsaedy, A.E. Alshorbagy, *Fib. Polym.*, **21**, 840 (2020)
33. M. Megahed, M.A. Abd El-baky, A.M. Alsaedy, A.E. Alshorbagy, *Fib. Polym.*, **22**, 1366 (2021)
34. A.I. Selmy, M.A. Abd El-baky, D.A. Hegazy, *J. Thermop. Compos. Mater.*, **32**, 267 (2018)
35. M.M. Awd Allah, M.A. Abd El-baky, M.A. Hassan, A. Shaker, *Fib. Polym.*, **23**, 3268 (2022)
36. S. Dhar Malingam, F.A. Jumaat, L.F. Ng, K. Subramaniam, A.F. Ab Ghani, *Advanc. Polym. Tech.*, **37**, 2385 (2018)
37. G.R. Rajkumar, M. Krishna, H.N. Narasimhamurthy, Y.C. Kes-havamurthy, J.R. Nataraj, *Proced. Mater. Sci.* **5**, 60 (2014)
38. H. Li, Y. Xu, X. Hua, C. Liu, J. Tao, *Compos. Struct.* **187**, 354 (2018)
39. N.R.J. Hynes, N.J. Vignesh, J.T.W. Jappes, P.S. Velu, C. Barile, M.A. Ali, M.U. Farooq, C.I. Pruncu, *Compos. Sci. Tech.*, **221** (2022)
40. Y. Hu, Y. Zhang, X. Fu, G. Hao, W. Jiang, *Compos. Struct.*, **229** (2019)

Springer Nature or its licensor (e.g. a society or other partner) holds exclusive rights to this article under a publishing agreement with the author(s) or other rightsholder(s); author self-archiving of the accepted manuscript version of this article is solely governed by the terms of such publishing agreement and applicable law.